Noise-memory induced excitability and pattern formation in oscillatory neural models

Erik Glatt, Hauke Busch,* and Friedemann Kaiser
Institute of Applied Physics, Darmstadt University of Technology, 64289 Darmstadt, Germany

Alexei Zaikin
Institut für Physik, Potsdam Universität, Am Neuen Palais 10, D14469 Potsdam, Germany
(Received 19 April 2005; published 22 February 2006)

We report a noise-memory induced phase transition in an array of oscillatory neural systems, which leads to the suppression of synchronous oscillations and restoration of excitable dynamics. This phenomenon is caused by the systematic contributions of temporally correlated parametric noise, i.e., possessing a memory, which stabilizes a deterministically unstable fixed point. Changing the noise correlation time, a reentrant phase transition to noise-induced excitability is observed in a globally coupled array. Since noise-induced excitability implies the restoration of the ability to transmit information, associated spatiotemporal patterns are observed afterwards. Furthermore, an analytic approach to predict the systematic effects of exponentially correlated noise is presented and its results are compared with the simulations.

DOI: 10.1103/PhysRevE.73.026216 PACS number(s): 89.75.Kd, 05.40.−a, 05.70.Fh

Pathological cerebral synchronization is able to perturb normal brain functions. This behavior plays an important role for some neural diseases such as Parkinson's disease or essential tremors [1]. In this context, it is important to find methods to suppress undesirable global oscillations in neural networks. Several techniques to achieve this have been reported, for example, high-frequency stimulation [2], phase resetting methods [1], or a delay-induced desynchronization [3]. A different method, which leads not only to the suppression of these unwanted dynamics, but also to *restoration* of excitable neural properties has been presented in [4], where multiplicative noise was used to stabilize the deterministically unstable fixed point of the local dynamics in an array of oscillatory systems. This noise-induced excitability (NIE) has been reported using FitzHugh-Nagumo (FHN) systems [5,6] with multiplicative white noise.

Increasing experimental evidence has established in recent years that *noise memory* can be important for neural communication and control of neural activity (e.g. [7,8]). Temporally correlated noise is supposed to be present in neural ensembles due to an intrinsic stochasticity of ion channels and other bioelectrical neural cell elements as well as due to the stochasticity of underlying synaptic communications (e.g., [9]). Massive spike trains received by cortical neurons effectively lead to correlated noise input, due to the low-pass frequency filtering effect of the synaptic dynamics [10–12].

In theory structured noise is also of great interest. Spatiotemporally correlated noise has interesting effects on pattern formation in excitable systems [13] and on the lifetime of scroll rings [14]. A transition to excitability in the presence of structured noise is reported in [15]. It is worth noting that, this noise-induced transition occurs not from the oscillatory regime, and the noise does not suppress the regular dynamics of the system. Furthermore the ability of correlated noise to induce a transition from random turbulence to regular waves was demonstrated in [16].

In our work, in contrast to [4], the noise is assumed to be structured in time, which leads to a new phenomenon. It is shown that noise memory can induce a reentrant phase transition that enhances the system's stability and restores an excitability, while preserving the overall phase-space structure. To demonstrate this noise-memory induced excitability (NMIE) an array of coupled oscillatory FHN systems under the influence of the multiplicative noise is studied.

Neurons with multiplicative responses are powerful computational elements in neural networks [17]. Multiplicative responses of a neural network stands for external parametric treatment or for internal communication responses reported, e.g., in the insect visual system [18], parietal cortex [19], or the superior colliculus [20]. Surprisingly, additional noise memory is critical for NMIE and leads to more disorder in the system, similarly to noise-induced phase transitions, as reported in [21,22]. To clarify if the growing correlation in time perturbs the effect of noise-suppressed dynamics, numerical simulations are performed with different correlation times. Finally, it is shown that noise memory is essential for the information transmission and pattern formation in this system. The simulations of NMIE are supported analytically by a small noise expansion (SNE) [23] with corrections for the temporally colored noise [24].

The system under consideration is an array of $N \times N$ coupled FHN systems in the presence of the parametric multiplicative noise $\eta_{ij}(t)$

$$\dot{u}_{ij} = \frac{1}{\mu}[u_{ij}(1-u_{ij})(u_{ij}-a) - v_{ij} + d_u] + q_u K_{ij},$$

$$\dot{v}_{ij} = u_{ij} - c(1+\eta_{ij})v_{ij}, \tag{1}$$

where K_{ij} and q_u denote the coupling function and strength, respectively. In this minimal model of neural dynamics $u_{ij}(t)$ represents the fast relaxing membrane potential, while $v_{ij}(t)$

*Permanent address: Division Theoretical Bioinformatics, German Cancer Research Center (DKFZ), 69120 Heidelberg, Germany.

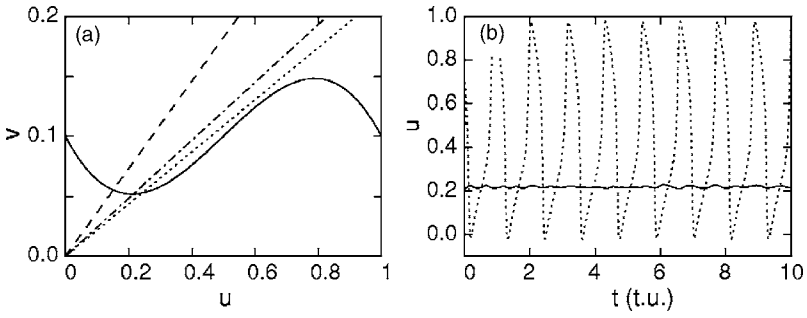

FIG. 1. (a) Nullclines in phase space (u,v) for noisy FHN system [Eq. (8)]. $(\cdot\ \cdot)$ $\sigma=0.0$, $(-\ \cdot\ -)$ $\sigma=1.5$, $(-\ -)$ $\sigma=3.0$. (b) mean field trajectories for Eq. (1) with global coupling [Eq. (11)] for $N=50, q_u=50$. $(\cdot\ \cdot)$ $\sigma=0.0$, (—) $\sigma=1.5$. Other parameters: $\tau=0.01$ t.u.

denotes the slow ion recovery variable, with the time scales being separated by the small parameter $\mu=0.01$. The time is specified in time units (t.u.), which accord approximately with the oscillation period of the net. The equations are integrated on a discrete spatiotemporal grid using the Heun method ($\Delta t=0.001$ t.u.) [23] and the forward time centered space scheme ($\Delta h=1.0$) in time and space, respectively. The grid points are labeled by the indices $1\leqslant i,j\leqslant N$. Throughout this paper the following set of parameters is used $(a,c,d_u)=(0.5,4.6,0.1)$, while varying the coupling strength q_u and the noise input η_{ij}. For $\eta_{ij}(t)=0$, each FHN system performs autonomous limit cycle oscillations, yielding a synchronized output in the case of $q_u>0$ and appropriate initial conditions.

The term $\eta_{ij}(t)$ is taken to be zero mean, spatially incoherent Gaussian noise of Ornstein-Uhlenbeck type with the correlation

$$\langle \eta_{ij}(t)\,\eta_{kl}(t')\rangle = \frac{\varepsilon}{\tau}\delta_{ij,kl}\exp(-|t-t'|\tau^{-1}), \tag{2}$$

where τ and ε denote the correlation time and the noise intensity, respectively [13,23]. This stochastic process fulfills the equation

$$\frac{\partial \eta_{ij}(t)}{\partial t} = -\frac{1}{\tau}\eta_{ij}(t) + \frac{1}{\tau}\xi_{ij}(t), \tag{3}$$

where $\xi_{ij}(t)$ is white Gaussian noise with $\langle \xi_{ij}(t)\xi_{kl}(t')\rangle = 2\varepsilon\delta_{ij,kl}\delta(t-t')$. The prefactor in Eq. (2) defines the noise variance of the Ornstein-Uhlenbeck noise $\sigma^2=\varepsilon/\tau$. In the following σ is denoted as noise strength. We believe, that for comparison with experimental systems the noise variance σ^2 is the relevant parameter, because for fixed σ^2 the total power of the noise is conserved. For that reason our theoretical and numerical studies are implemented with fixed σ and hence fixed σ^2.

A small noise expansion is used in order to predict the systematic effect of the parametric fluctuations on the system behavior [23]. For the case of a stochastic differential equation $\dot{x}(t)=f(x(t))+g(x(t))\,\eta(t)$, the first order of the expansion reads

$$\dot{x}_0(t) = f(x_0(t)) + \langle g(x_0(t))\,\eta(t)\rangle_t, \tag{4}$$

where the temporal mean can be evaluated using Novikov's theorem [25]

$$\langle g(x(t))\,\eta(t)\rangle = \int_0^t dt'\,\sigma^2\exp(-|t-t'|\tau^{-1})\left\langle g'(x(t))\frac{\delta x(t)}{\delta\eta(t')}\right\rangle. \tag{5}$$

It is possible to obtain an analytical approximation for the individual system's response to the noise in the limit of short-memory stochastic forcing using a Taylor expansion with respect to time [24]. One obtains

$$\frac{\delta x(t)}{\delta\eta(t')} \approx g(x(t)) + g^2(x(t))\left(\frac{f(x(t))}{g(x(t))}(t'-t)\right), \tag{6}$$

which leads to the final expression for the SNE up to first order

$$\dot{x}_0(t) \approx f(x_0(t)) + \sigma^2 g'(x_0(t))g(x_0(t))\left[\tau + g(x_0(t)) \times\left(\frac{f(x_0(t))}{g(x_0(t))}\right)'\tau^2\right]. \tag{7}$$

This new combination of known results leads to a useful tool to predict deterministic effects of structured multiplicative noise of Ornstein-Uhlenbeck type, as will be demonstrated for the FHN system in the following.

While the assumptions of the SNE strictly hold for an individual system, only, the analysis is also valid for strongly coupled networks of oscillators. The systematic effect of the parametric forcing already appears on the level of the individual oscillator, while the role of coupling is to dampen short-term local fluctuations, this way establishing the respective noise-induced dynamic regimes. With these prerequisites in mind, the estimation of Eq. (1) up to the first order, using Eq. (7), reads

$$\dot{u}_{ij} = \frac{1}{\mu}[u_{ij}(u_{ij}-1)(a-u_{ij}) - v_{ij} + d_u] + q_u K_{ij},$$

$$\dot{v}_{ij} = u_{ij} - cv_{ij} + \sigma^2 c^2(v_{ij}\tau - u_{ij}\tau^2). \tag{8}$$

The predicted deterministic effect of increasing multiplicative noise on the single, uncoupled system for $\tau=0.01$ t.u. is depicted in Fig. 1. In the absence of noise ($\sigma=0$), the system is oscillatory and the trajectory follows a limit cycle. Increasing the noise strength for small τ tilts the linear nullcline to the left according to

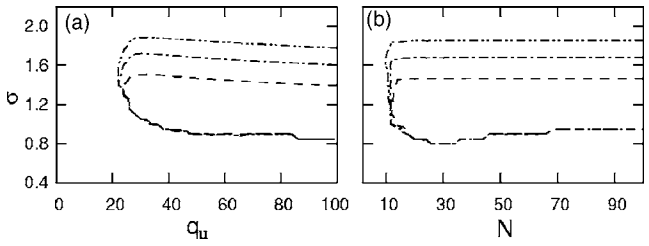

FIG. 2. Boundaries of NMIE for Eq. (1) with global coupling [Eq. (11)]. (a) coupling strength q_u vs noise strength σ, $N=50$. (b) system size N vs noise strength σ, $q_u=50$. Contour lines: (– · · –) RRT=0.97, (– · –) RRT=0.98, (– – –) RRT=0.99. Other parameters: $\tau=0.01$ t.u.

$$v(u) = \frac{\sigma^2 c^2 \tau^2 - 1}{\sigma^2 c^2 \tau - c} u = mu, \tag{9}$$

which causes the unstable fixed point to move towards the stable branch of the cubic nullcline [Fig. 1(a)]. Using this result one finds the following relation between the noise strength σ, the slope of the linear nullcline m, and the noise-memory τ

$$\sigma(\tau, m) = \frac{1}{c} \sqrt{\frac{1 - cm}{\tau(\tau - m)}}. \tag{10}$$

For a slope $m \gtrsim 0.224$ the fixed point becomes stable, thus according to Eq. (10) noise amplitudes $\sigma \gtrsim \sigma_{fi}(\tau=0.01) \approx 0.82$ are required to suppress the oscillatory dynamics. Consequently the oscillations in the globally coupled array can be suppressed using parametric noise [Fig. 1(b)]. For $\sigma_{st}(\tau=0.01)=(c\tau)^{-1/2} \approx 4.66$ the linear nullcline of Eq. (8) is vertical, while for $\sigma > \sigma_{st}$ the former stable fixed point becomes unstable once more.

Next, we consider a globally coupled array of FHN systems [Eq. (1)] with coupling function defined as

$$K_{ij} = \bar{u} - u_{ij}, \tag{11}$$

where $\bar{u}$ denotes the mean value of the fast variable for all systems (mean field). To show the existence of NMIE in a globally coupled array, we calculate the relative resting time (RRT) of all systems in a confined phase-space area close to the fixed point ($u_{ij} < 0.35$ and $v_{ij} < 0.1$). The array is assumed to display NMIE, if RRT > 0.98 [4].

The RRT for Eq. (1) with global coupling is plotted in Fig. 2. Obviously, a minimum coupling strength $q_u \approx 24$ is necessary to bind the mean field to the noise-induced stable fixed points [Fig. 2(a)], i.e., to establish NMIE. Furthermore, the border noise strength (σ_{fi}) between the oscillatory and NMIE regime, is monotonously decreasing with growing coupling strength q_u approaching the value predicted from Eq. (10). Similarly, a minimum system size $N \approx 10$ is required to observe NMIE [Fig. 2(b)]. Interestingly, σ_{fi} shows a resonant behavior with the system size, being minimal for $N \approx 30$. These results clearly show that NMIE is a collective behavior. In a single noisy FHN system the fluctuations dominate the systematic noise effects [Eq. (8)], while these fluctuations can be minimized using large arrays of such systems and strong coupling.

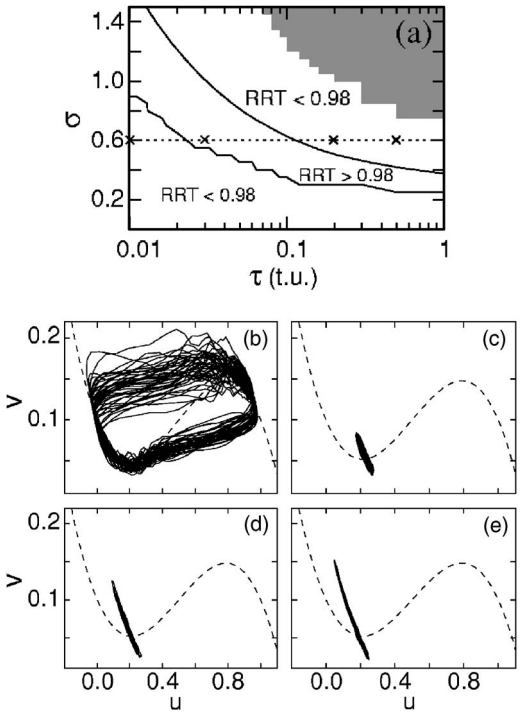

FIG. 3. (a) boundaries of NMIE for Eq. (1) with global coupling [Eq. (11)] as a function of the noise strength σ and correlation time τ, $N=50$, $q_u=50$. (· · ·) marks $\sigma=0.6$. (b)–(e) trajectories in phase space (u,v), associated with crosses in (a), at $\sigma=0.6$, (b) $\tau=0.01$ t.u., (c) $\tau=0.03$ t.u., (d) $\tau=0.2$ t.u., and (e) $\tau=0.5$ t.u. (- – –) cubic nullcline of Eq. (1). The gray area in (a) marks the values of τ and σ, where the numerical integration with fixed Δt becomes unstable for $\sigma(\tau) > \sigma_{st}(\tau)$.

The upper boundary of the NMIE regime (σ_{ub}) is established by the fact that an increasing noise strength leads to a shift of the fixed point towards larger values of the v variable as well as to larger overall fluctuations, resulting in an effective decrease of the RRT with σ. For noise intensities greater than $\sigma_{st}(\tau)$, the numerical integration becomes unstable as a consequence of the change of stability of the fixed point, as predicted from Eq. (8).

Varying the noise memory, one observes a growing disturbance of the transition to NMIE with increasing noise memory. From Fig. 3(a) one finds NMIE in the full examined range of τ. Increasing the noise memory results in a shift of the NMIE regime towards smaller values of σ. Surprisingly, increasing the correlation time τ of the noise leads to the decrease of the area in which oscillations are suppressed, similarly to noise-induced phase transitions via short time instability [21,22]. This renders NMIE a much different phenomenon as compared to *asynchronous oscillation suppression*, widely known in the theory of oscillations [26]. The corresponding trajectories of the mean field, which illustrate the change of the order parameter RRT on the noise memory, are shown in Figs. 3(b)–3(e). First, oscillations are suppressed by noise, giving rise to NMIE [Fig. 3(c)]. Increasing the noise memory further results in large fluctuations of the v variable, destroying the σ-associated NMIE regime [Figs. 3(d) and 3(e)].

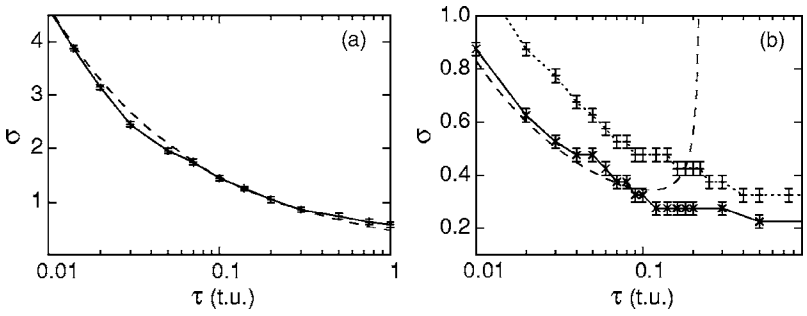

FIG. 4. Comparison of critical noise strengths from SNE [Eq. (8)] (– – –) and simulation of Eq. (1) with global coupling [Eq. (11)]. (a) $\sigma_{st}(\tau)$ at $q_u=50$. (b) $\sigma_{fi}(\tau)$: (···) $q_u=25$, (—) $q_u=50$. (—), (···) connect the numerical results. Other parameters: $N=50$.

Comparing the analytical prediction [Eq. (10)] for $\sigma_{st}(\tau)$ from SNE [Eq. (8)] with the numerical results shows excellent agreement for the whole range of noise memory [Fig. 4(a)]. The monotonous decrease of σ_{st} with τ also explains the shift of the numerically intractable parameter region of NMIE towards smaller noise strengths with increasing noise memory in Fig. 3(a). The predictions of $\sigma_{fi}(\tau)$ from the SNE approximation and the numerical solutions, however, diverge for weak coupling ($q_u<40$) and large $\tau\gtrsim 0.1$ t.u. [Fig. 4(b)]. Once again, these results reflect the fact that NMIE is a collective phenomenon and, moreover, that a higher order Taylor expansion for the derivation of the SNE is needed to account for long-range noise-memory effects in the stochastic dynamics.

In order to study the pattern formation and the signal transmission through the array, the function K_{ij} in Eq. (1) is chosen as diffusive nearest-neighbor coupling with periodic boundary conditions, using a nine-point Laplacian for radial symmetry

$$K_{ij} = \nabla^2 u_{ij},$$

$$\nabla^2 u_{ij} = \tfrac{1}{6}[u_{i+1,j+1} + u_{i+1,j-1} + u_{i-1,j+1} + u_{i-1,j-1} + 4(u_{i+1,j} + u_{i-1,j} + u_{i,j+1} + u_{i,j-1}) - 20u_{i,j}]. \quad (12)$$

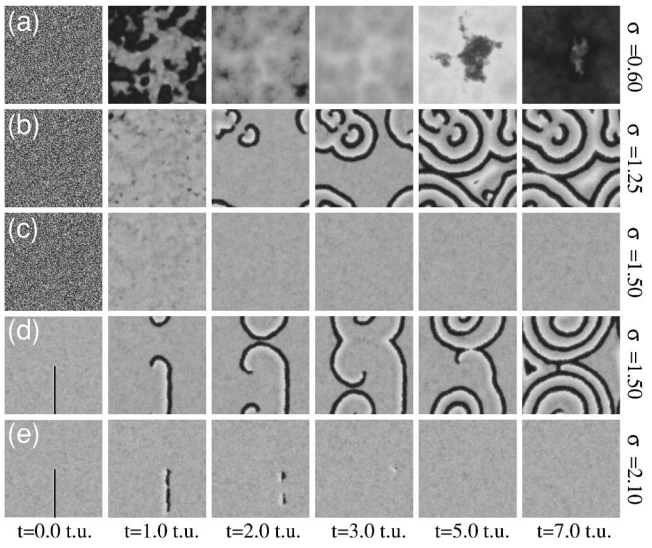

FIG. 5. Snapshots of $u(t)$ for Eq. (1) with diffusive coupling [Eq. (12)]. (a)–(c) random initial conditions; (d) and (e) initial conditions induce two spiral waves in an excitable system. Other parameters: $N=256$, $q_u=50$, $\tau=0.01$ t.u.

Three different pattern forming regimes are expected to appear with increasing noise strength. For $\sigma(\tau)<\sigma_{fi}(\tau)$, the array elements oscillate, while for $\sigma_{fi}(\tau)<\sigma(\tau)<\sigma_{ub}(\tau)$, the excitable dynamics of each element are predominant in the NIE regime and typical spatiotemporal patterns such as spiral waves appear. Finally, for $\sigma_{ub}(\tau)<\sigma(\tau)<\sigma_{st}(\tau)$, a noise-induced subexcitable regime (NMISE) is reached, in which spatiotemporal patterns are no longer supported and any initial excitation dies out for $t\to\infty$. Figure 5 depicts the numerical simulation results for a diffusively coupled array. For $\sigma=0.6$ global oscillations are observed, which become ever more synchronized over time due to the spatial coupling [Fig. 5(a)]. For $\sigma=1.25$, the system is in the NMIE regime and excitable dynamics prevail, as visible from the spatial structures [Fig. 5(b)]. Increasing the noise strength restores the excitability of the individual array elements and helps information transmission (see also other mechanisms of noise-increased information transmission [27,28]). Consequently, the array approaches a global attractor most of the time, if starting from random initial conditions [Fig. 5(c)]. Nevertheless, spiral waves are still fully supported, if appropriate initial conditions are chosen [Fig. 5(d)]. For $\sigma=2.1$ the NMISE regime is reached, and spatial patterns die out regardless of the initial conditions [Fig. 5(e)].

Snapshots of the diffusively coupled array for increasing noise strength and memory are presented in Fig. 6. Clearly,

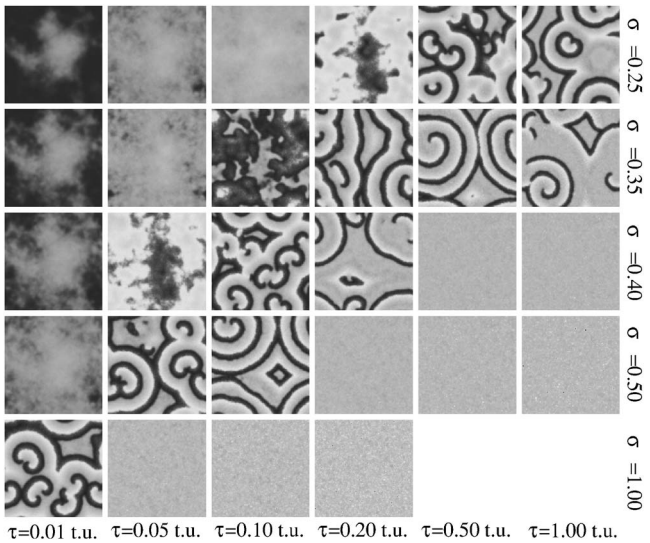

FIG. 6. Snapshots of $u(t)$ for Eq. (1) with diffusive coupling [Eq. (12)] taken at $t=10.0$ t.u. Simulations started with random initial conditions. Other parameters: $N=256$, $q_u=50$.

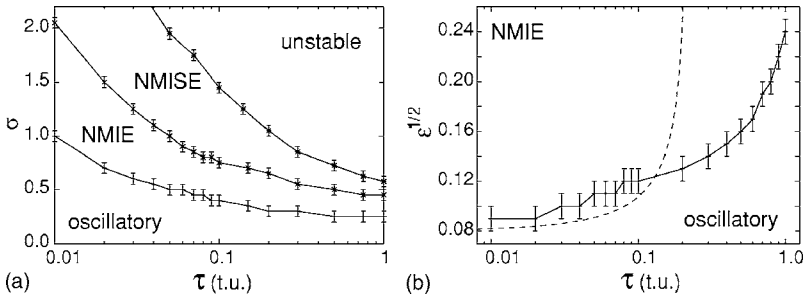

FIG. 7. (a) Pattern forming regimes for Eq. (1) with diffusive coupling [Eq. (12)] as a function of noise strength σ and noise correlation time τ. (b) Transition oscillatory regime to NMIE as a function of noise intensity ε and noise correlation time τ. (—) connect the numerical results, (– – –) theoretical prediction [Eq. (8)]. Other parameters: $N=256$, $q_u=50$.

the occurring types of spatiotemporal patterns are the same in the examined range of τ. However, the onset of the structure forming NMIE regimes is shifted to smaller noise strengths with increasing τ, quite in agreement with the results from the globally coupled array. The visual impression from Fig. 6 is summarized in Fig. 7(a). There, the various dynamic regimes have been systematically analyzed from the observed spatiotemporal patterns. The expected monotonous decrease of $\sigma_{fi}(\tau), \sigma_{ub}(\tau)$, and $\sigma_{st}(\tau)$ with τ is clearly visible. The NMIE region corresponds perfectly with the one for the globally coupled array from Fig. 3.

The monotonous decrease of the various dynamical regimes towards smaller noise strengths σ with increasing noise-memory τ can be understood qualitatively in terms of the frequency-response matching between the stochastic forcing and the intrinsic time scale individual FHN system. The total power of the noise depends on the noise strength σ, whereas the power spectral density (PSD) obviously depends on the noise-memory τ. Increasing the latter leads to an ever increasing correlation between the PSD of the noise and the frequency response of the FHN systems, thus resulting in the observed dependence of the transitions to NMIE with τ.

For the sake of completeness, Fig. 7(b) shows the border between the oscillatory regime and NMIE as a function of the noise intensity ε. Numerical evidence suggests that the border depends on τ, as is clearly visible for $\tau \gtrsim 0.1$ t.u. For smaller values of the correlation time the observed dependence is in good agreement with the analytical approximation from Eq. (10), but is not strongly pronounced. For $\tau \lesssim 0.01$ t.u. the border becomes a horizontal line and converges against the white noise result.

In summary, it has been shown that noise memory induces reentrant phase transitions from oscillations to excitability in a global coupled array of FHN systems with parametric time correlated noise. This transition is stable for a wide parameter range of noise correlation times. In contrast to other suppression techniques, spatial coupling is absolutely essential in this case, in order to prevent noise-driven oscillations from exciting the system and converting it back in an oscillator. Using a nonstandard SNE the observed effects have been successfully approximated even for temporally correlated noise, providing good predictions for the observed system for not too large noise memory.

Applying diffusive coupling, the NMIE regime was found in the expected range of $\sigma(\tau)$ and the corresponding spatiotemporal patterns were observed. Increasing the noise strength shifts the system's dynamics from the oscillatory to the excitable regime, thus allowing for pattern formation and subsequent information transmission at intermediate σ and τ. Furthermore, the existence of a NMISE regime was proved for $\sigma_{ub}(\tau) < \sigma(\tau) < \sigma_{st}(\tau)$. It has been demonstrated that optimal memory of the noise is essential to observe spiral pattern formation, as the phase boundaries of the NMIE and NMISE regimes crucially depend on the noise correlation time.

NMIE was studied using the paradigmatic FHN model in a rather general framework. We hope that these theoretical findings will not only contribute to the theory of extended systems with noise [23] but also help to develop new strategies to suppress malfunction neural oscillations, restore the functionality of neural networks, as well as to understand the functionality of coupled neurons that form multiplicative representations in evolutionary adapted systems, including previously reported examples in the superior colliculus [20], the lateral intraparietal area [19], or the insect visual system [18].

A.Z. acknowledges financial support from VW-Stiftung (Germany).

[1] P. A. Tass, *Phase Resetting in Medicine and Biology. Stochastic Modelling and Data Analysis* (Springer, Berlin, 1999).
[2] A. Benabid, P. Pollack, and C. Gervason, Lancet **337**, 403 (1991).
[3] M. G. Rosenblum and A. S. Pikovsky, Phys. Rev. Lett. **92**, 114102 (2004).
[4] E. Ullner, A. Zaikin, J. García-Ojalvo, and J. Kurths, Phys. Rev. Lett. **91**, 180601 (2003).
[5] J. S. Nagumo and S. Yoshizawa, Proc. IRE **50**, 2061 (1962).
[6] R. A. FitzHugh, Biophys. J. **1**, 445 (1961).
[7] D. Nozaki, D. J. Mar, P. Grigg, and D. J. Collins, Phys. Rev. Lett. **82**, 2402 (1999).
[8] B. Doiron, B. Lindner, A. Longtin, L. Maler, and J. Bastian, Phys. Rev. Lett. **93**, 048101 (2004).
[9] J. White, R. Klink, A. Alonso, and A. Kay, J. Neurol. **80**, 262 (1998).
[10] N. Brunel and S. Sergi, J. Theor. Biol. **195**, 87 (1998).
[11] N. Fourcad and N. Brunel, Neural Comput. **14**, 2057 (2002).
[12] Y. Sakai, S. Funahashi, and S. Shinomoto, Neural Networks **12**, 1181 (1998).

[13] H. Busch and F. Kaiser, Phys. Rev. E **67**, 041105 (2003).
[14] V. Pérez-Muñuzuri, F. Sagués, and J. M. Sancho, Phys. Rev. E **62**, 94 (2000).
[15] S. Alonso, F. Sagués, and J. M. Sancho, Phys. Rev. E **65**, 066107 (2002).
[16] S. Alonso, J. M. Sancho, and F. Saguès, Phys. Rev. E **70**, 067201 (2004).
[17] E. Salinas and L. Abbot, Proc. Natl. Acad. Sci. U.S.A. **93**, 11956 (1996).
[18] N. Hatsopoulos, F. Gabbiani, and G. Laurent, Science **270**, 1000 (1995).
[19] R. Andersen, R. Bracewell, S. Barash, J. Gnadt, and L. Fogassi, J. Neurosci. **10**, 1176 (1990).
[20] A. Van Opstal, K. Hepp, Y. Suzuki, and V. Henn, J. Neurophysiol. **74**, 1593 (1995).
[21] S. Mangioni, R. Deza, H. S. Wio, and R. Toral, Phys. Rev. Lett. **79**, 2389 (1997).
[22] S. E. Mangioni, R. R. Deza, R. Toral, and H. S. Wio, Phys. Rev. E **61**, 223 (2000).
[23] J. García-Ojalvo and J. M. Sancho, *Noise in Spatially Extended Systems* (Springer, New York, 1999).
[24] J. M. Sancho, M. San Miguel, S. L. Katz, and J. D. Gunton, Phys. Rev. A **26**, 1589 (1982).
[25] E. A. Novikov, Sov. Phys. JETP **20**, 1920 (1964).
[26] P. Landa, *Nonlinear Oscillations and Waves in Dynamical Systems* (Kluwer Academic, Dordrecht, 1996).
[27] L. Gammaitoni, P. Hänggi, P. Jung, and F. Marchesoni, Rev. Mod. Phys. **70**, 223 (1998).
[28] M. C. Eguia, M. I. Rabinovich, and H. D. I. Abarbanel, Phys. Rev. E **62**, 7111 (2000).